Lunar Explorers - Spacecraft Operations Proposal

Guerrero Hernández, Aníbal
Chair of Pico and Nano Satellites (PNS)
Technical University of Munich (TUM)
Munich, Germany
03771704
anibal.guerrero@tum.de

Thepdawala, Sibtain Ali
Chair of Pico and Nano Satellites (PNS)
Technical University of Munich (TUM)
Munich, Germany
03779317
sibtainali.thepdawala@tum.de

CONTENTS

List of Tables

List of Figures

I. Mission Statement & Objectives

Asteroid mining seems like a distant dream. In essence, great technological and financial difficulties lie between the present and a future were asteroids can be exploited. With the mission presented by *Lunar Explorers*, the fictious scenario becomes more real, as steps are taken towards it.

To develop technology, financial aid is required. For financial aid to be received, technology must be developed. This leads to the paradox of the ouroboros [11]. For this reason, technology has to be demonstrated before financial investors start pouring money into the industry. They require assurance that a project is viable. The idea behind the *Lunar Explorers* mission is to break the vicious cycle with a technology demonstrator on the Moon.

Asteroids and comets possess water reserves and Platinum-Group Metals (PGMs) that are scarce on Earth. Water can be converted into O_2 for life support systems, and H_2 for refuelling spacecrafts, reducing the ΔV requirements for going to Space. The focus of *Lunar Explorers*is the collection of H_2O for oxygen extraction and utilisation in life support systems such as those implemented in the ISS and future concepts.

A. Primary Objective

To demonstrate the technology required to retrieve samples of volatile materials, such as water ice and organic compounds from asteroids, from a crater on the Moon with similar water concentrations.

B. Secondary Objectives

1) **Push towards ISRU:** Initiate efforts to make spacecrafts that can utilise resources extracted outside of Earth.
2) **Space Infrastructure and Lunar Base:** The construction of a *Lunar Base* is an essential milestone towards generating space infrastructure and enabling a wider use of Space to a general public and commercial actors that currently are behind an economic barrier.

C. Expected Deliverables from the Mission

1) **Space Mining Technology Demonstration:** Demonstration of innovative space mining technology, including robotic extraction rovers and ore retriever rockets, tailored for resource extraction from the Moon.
2) **Scientific Analysis and Research Findings:** Analysis of retrieved samples and scientific data to advance understanding of the Moon's composition and origin, leading to scientific publications and further exploration efforts.
3) **Composition Analysis of Mined Regolith:** Detailed analysis of the composition of mined regolith from the Moon to assess its suitability for resource utilization in future space missions, contributing to the development of sustainable space exploration strategies.
4) **Ore-Retriever Development:** Designing and validation of a secure sample ore-retriever for transporting volatile materials from the Moon.
5) **Navigation System:** Validation of an advanced navigation system, enabling precise spacecraft maneuvering and approach to the Moon for resource extraction.
6) **Reliable Communication Link:** Establishing a communication system to ensure continuous connectivity between the spacecraft and the ground station, facilitating seamless transmission of mission data, telemetry, and commands.

II. STK Simulation

A. Concept of Operations

The spacecraft is separated into modules:

- **L**: Launcher - not part of the spacecraft but responsible for launching to LEO.
- **OM**: Observation Module - module with payload cameras, responsible for imagery and general observation strategies. (*Not considered in detail within this project*)
- **MM**: Main Module - contains the mining payload to be deployed to the Moon.
- **ER**: Extraction Rover - mining payload responsible for regolith extraction.
- **OR**: Ore Retriever - regolith storage unit (where ER deposits regolith).

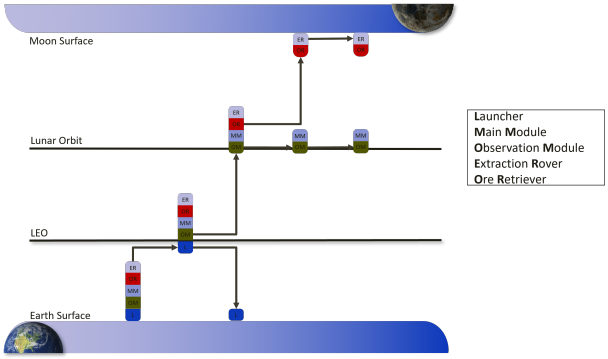

Fig. 1: *Lunar Explorer*'s Concept of Operations consists of four phases - Launch to LEO, Transfer to Lunar Orbit, Orbit around the Moon, and Lunar Descent.

Lunar Explorer's concept of operation is the following:

1) **Launch**: The Starship launcher takes the spacecraft to space, as represented in Figure 4, where the spacecraft will deploy and start the deployment sequence as shown in Figure 7.
2) **Travelling to a Lunar Orbit**: The *OM* will transport the spacecraft to a lunar orbit, at which point it will perform observation duties while the mission carries on in parallel. Further details are addressed in Figure 10
3) **Lunar Orbit**: The spacecraft is captured by the Moon after an impulsive maneuver, described in Figure 9. The *MM* now takes charge of the propulsive requirements, carrying out any corrective maneuvers for the spacecraft's attitude in the lunar orbit. These are detailed in Figure 10. The objective is that the spacecraft orientates itself into a position and orientation optimal for *ER* and

OR deployment for later descent. Further details are addressed in Figure 12

4) **Mining Modules Landing**: *ER* and *OR* land on the Moon's surface after the last impulsive maneuver, Figure 11. For the time required to obtain the desired regolith mass, mining will occur on the surface of it. After mining is completed, the *OR* will return to the *MM* that was in a lunar orbit, waiting for the module that contains the regolith samples collected. The *ER* will remain on the Moon.

B. Mission Control Sequence

Earth-to-Moon transfer can be described in four major phases, as mentioned below and visualized in Figure 2.

- Launch and Initial Orbit (Earth)
- Interplanetary transfer to the proximity of the Moon (TLI)
- Final Orbit around Moon (LOI)
- Descent Orbit Insertion (DOI) and Landing

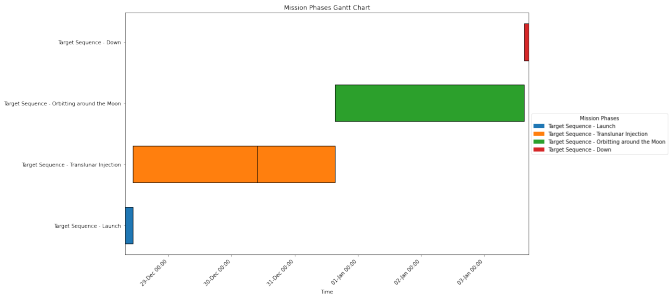

Fig. 2: Timeline for the different phases of the mission

1) Launch Strategy: This mission aims to utilize the capabilities of the Starship to achieve a *Low Earth Orbit* (LEO). According to several sources, this new launcher will be readily available by the end of 2024 [23]. By leveraging the performance and flexibility of the Starship, reliable and cost-effective access to space for this mission is ensured. The fully reusable nature of the Starship also contributes to reducing launch costs and increasing accessibility to space.

The launch strategy consists of launching with the Starship from SpaceX's Cape Canaveral Site in Florida, USA. An illustration of a Starship mounted onto the launch tower is represented in Figure 3.

TABLE I: Technical Information on Launch Opportunity.

Parameter	Value	Unit
Operator	SpaceX	-
Launcher	Starship	-
Launch Location	Cape Canaveral, Florida, USA	-
Launch Date	28th December 2024 [8]	-
Orbit	LEO	-
Available Payload	100	t
Latitude	28.39	°N
Longitude	80.6	°W
Ground Stations	Deep Space Network (DSN)	-

Fig. 3: SpaceX's Starship mounted to their launch tower at Cape Canaveral, FL.

As the spacecraft considered for this mission is composed of several modules, but designed to fit inside Starship's fairing volume and weight constraints, just a single launch is required to fully deploy all relevant components of the mission. Further information on the structural considerations and integration can be consulted in subsection V-D respectively.

TABLE II: Initial Low Earth Orbit Parameters

Eccentricity	Altitude [km]	Inclination [°]	Period [min]
0	275	28.40°	90

Ansys Systems Tool Kit (STK) provides a physics-based modeling environment for analyzing platforms and payloads in a realistic mission context. As illustrated in Figure 4, the launch and coast phases have been simulated taking into account the launch site and spacecraft.

2) Deployment Sequence: The deployment sequence of the whole satellite can be described in the following order of steps:

1) **Launcher separation:** Once the launcher reaches LEO, the satellite is deployed into orbit. This can be observed in 4d
2) **Detumbling:** The satellite uses its ADCS system to stabilize its attitude.
3) **Solar array deployment:** Once stabilized, the solar panels are deployed and all power-dependent subsystems are activated for status checks.
4) **Antenna deployment and communication:** The antenna reflector will be deployed and pointing tests will be done. Communication using both the X and the Ka-band antennas will be tested.
5) **Health check and telemetry:** The spacecraft will communicate with the ground and provide information about the state of each subsystem.

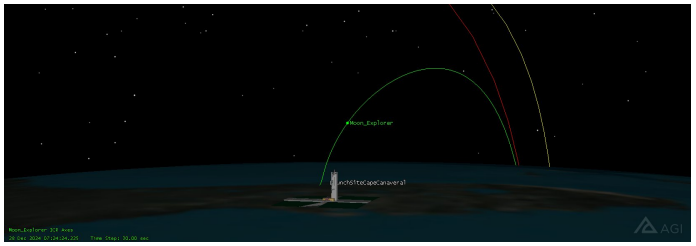

(a) Initial launch from Cape Canaveral. A view of the launch site is exaggerated for visualization purposes.

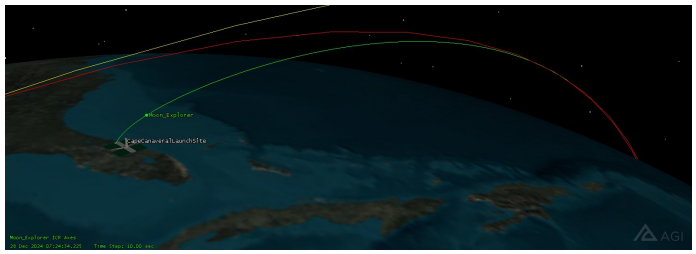

(b) Launch view from above, initial moments after departing launch site.

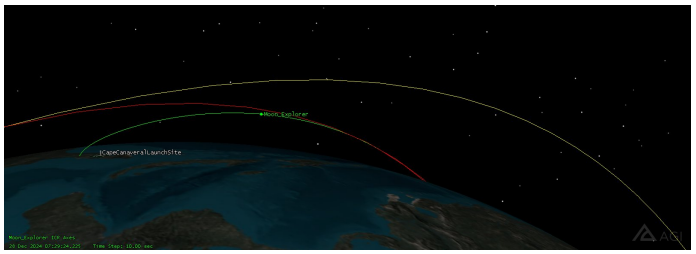

(c) Final moments before transitioning from launch to coasting, following the deployment sequence and separating from the launcher.

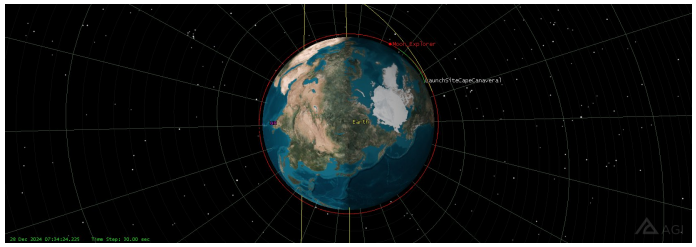

(d) *Lunar Explorer* in LEO Orbit after deployment sequence completed and coast phase achieved.

Fig. 4: **STK Launch Segment**: View of orbital trajectory followed by Starship in sequential order followed in (a), (b), (c), and a view of the LEO orbit achieved in (d). The green line represents the initial launch phase, whereas the red line represents the coasting phase around Earth.

6) **Hold:** The spacecraft will await a command from the ground station to proceed with the mission if everything looks nominal.
7) **Escape burn:** If every subsystem is working properly, the spacecraft waits for its next perigee to perform a Translunar Injection towards the desired interplanetary orbit to the Moon as illustrated in Figure 8 and its subsequent figures.

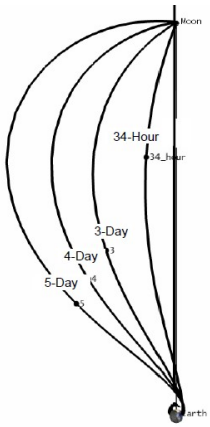

Fig. 5: Ballistic Transfers in Earth-Moon Rotating Coordinates

3) 4-Day Ballistic Transfer To Lunar Parking Orbit: The chosen trajectory for the mission under consideration entails a 4-day transfer from Earth to the Moon, depicted in Figure 5 and Figure 6. This trajectory closely mirrors the paths taken during the Apollo missions. A multi-profile targeting sequence was employed to design this trajectory, allowing for precise planning and optimization of the spacecraft's path.

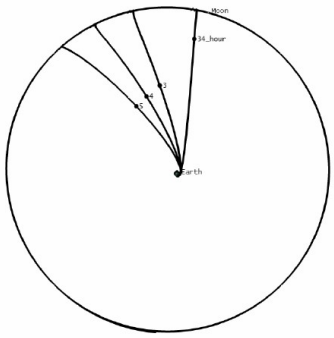

Fig. 6: Ballistic Transfer is Earth-Centered Inertial Coordinates

After the initial launch phase and subsequently reaching the LEO parking orbit around Earth, as explained in subsubsection II-B1. The coasting phase leads to the interplanetary transfer between Earth and the Moon, as observed in 4d. This is represented by the yellow line and occurs after an impulsive maneuver corresponding to the Trans-Lunar Injection (TLI). Further representation is illustrated in Figure 7, where the Moon, Earth, and full trajectory can be observed.

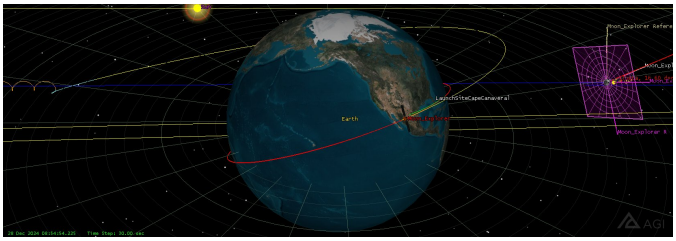

Fig. 7: Trans-Lunar Injection (TLI) maneuver. Transition from Low Earth Orbit to Lunar trajectory.

Using a first guess for the initial TLI maneuver based on previous studies (ΔV=3.12 km/s), the Launch (4b, 4b, 4c) and Coast were varied so that when the spacecraft was at approximately Lunar orbit distance - which corresponds to 300,000 km from Earth - the difference between the spacecraft's *Right Ascension* and *Declination* compared to those of the Moon are *zero*. We call this "Δ-RA" and "Δ-Dec" targeting. When this targeting profile has converged, then the Launch time, Coast time, and TLI ΔV are simultaneously adjusted to achieve a guess at the B-Plane parameters B·T and B·R ($-5,000$ km and $5,000$ km, respectively), as well as time of flight.

Subsequently, adjustments were made to the launch-coast-burn parameters to attain specific orbital characteristics. These adjustments aimed to achieve a periselene altitude of 668.23 km, an inclination of 83.32°, and a time-of-flight of 4 days. The chosen 4-day duration is approximately optimal, as it minimizes the required TLI and LOI ΔV. Following this adjustment, the Lunar Orbit Insertion (LOI) maneuver was targeted to establish a circular Lunar parking orbit, maintaining the same altitude of 668.23 km with a period of approximately 165 minutes. Refer to Table III for a detailed breakdown of the orbital parameters and Figure 10 & Figure 9 for insightful illustrations.

TABLE III: Final Lunar Orbit Parameters

Parameters	Values
Eccentricity	0.071185
Inclination [°]	83.32°
Altitude [km]	668.23
RAAN [°]	350.71°
Time Period [min]	165°

Following the Lunar Orbit Insertion (LOI) as illustrated in Figure 9, the spacecraft is inserted into a lunar orbit. The spacecraft remains in a parking lunar orbit for 3 days as shown in Figure 10. During this period, the trajectory aligns over the designated landing site, initiating preparations for the subsequent descent phase. The descent phase encompasses the Descent Orbit Insertion (DOI) maneuver, which precedes the powered descent to the lunar surface.

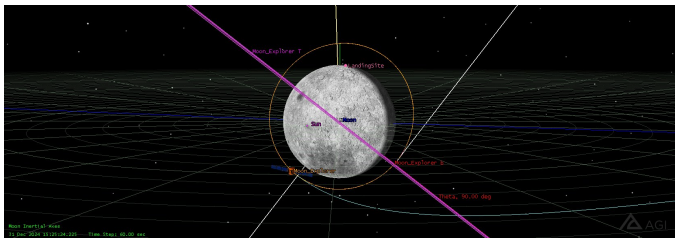

Fig. 9: *Lunar Orbit Injection (LOI)* maneuver. Transition from Interplanetary Lunar Transfer to Lunar Orbit.

It is important to point out that the descent phase is only undergone by the ore-retriever carrying the extraction rover while the main spacecraft continues to stay in the lunar orbit. However, for representation purposes and because the implementation of the spacecraft design developed in Figure 22 has not yet been accomplished for STK, the same representation for the spacecraft has been used to demonstrate the modules that would descend. This descent sequence entails a total ΔV requirement of 1319 m/s. For a comprehensive overview of this trajectory, including its major features and corresponding ΔV requirements, please refer to Table IV.

TABLE IV: Mission Summary: 5-Day Transfer to Lunar Orbit

Maneuver	**ΔV [m/s]**
Translunar Injection (TLI)	3,120.00
Lunar Orbit Insertion (LOI)	800.00
Down Landing Maneuver & Powered Descent (DOI)	1,391.28
Total ΔV	**5,311.28**

III. Alternate Architectures

This section provides insight into different trajectory approaches that can be utilized for carrying out the mission under consideration [10]. The major parameters of consideration are the time of flight and the total ΔV requirement to reach the lunar orbit. These trajectories are categorized as follows.

A. 3.5 Phasing Loop

To expand the launch window, several missions have added phasing loops before the final transfer from the Earth to the Moon. This can be used to adjust orbit period with perigee maneuvers to allow for more launch days per month while maintaining the same arrival day (to meet lunar lighting conditions.) An example with 3½ phasing loops is shown in Figure 13. The method is very similar to the 4-day transfer, except that a maneuver at the 3rd perigee (P3), just before the final transfer to the Moon, is needed to raise the apogee to

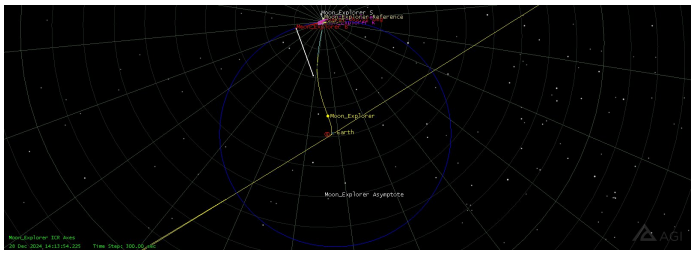

(a) Interplanetary 4-Day Transfer from Earth to the Moon in Earth-Moon Rotating Coordinates, centered on Earth. The blue line represents the Moon's orbit around Earth.

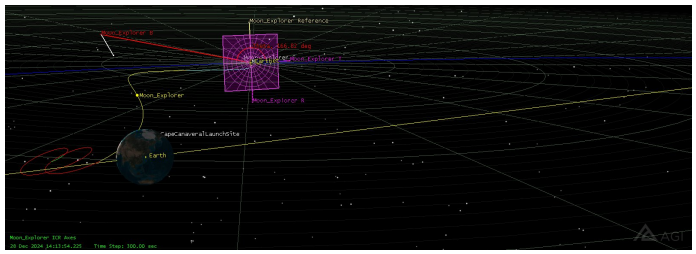

(b) Interplanetary 4-Day Transfer from Earth to the Moon in Earth-Moon Rotating Coordinates, zoomed in. Transfer is shown in yellow, whereas coast and lunar insertion are represented in red and blue respectively.

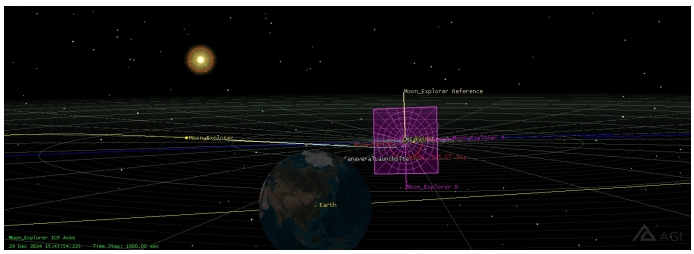

(c) Final moments before transitioning from launch to coasting, following the deployment sequence and separating from the launcher.

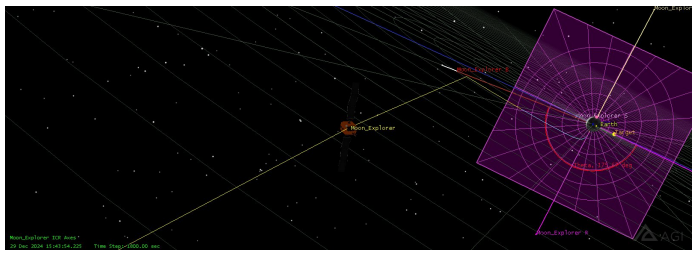

(d) *Lunar Explorer* in 4-Day Transfer Orbit after a successful TLI, approximating Moon. The Moon's B-Plane is represented in purple.

Fig. 8: **STK Interplanetary Transfer Orbit Segment**: View of orbital trajectory from TLI to Lunar Orbital Insertion (LOI). Overall trajectory contemplated in (a), zoomed in for (b) and (c). Views are provided in a sequential time order.

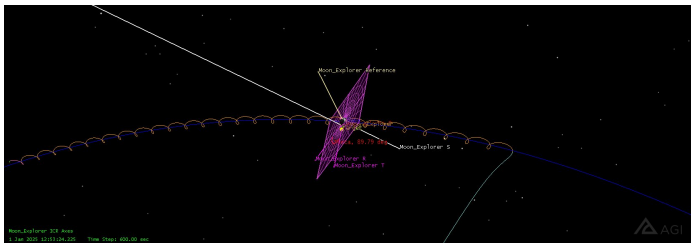

(a) *Lunar Explorer* orbiting around the Moon. LOI maneuver can be observed when the trajectory transforms from blue to orange.

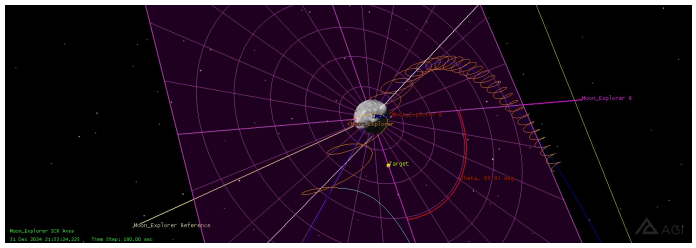

(b) *Lunar Explorer* orbiting around the Moon from a different angle, closer to the Moon as central body. DOI maneuver can be observed when the trajectory transforms from orange to green and the spiraling trajectory ends.

Fig. 10: **STK Lunar Orbit Segment**: View of Lunar Orbit trajectory from LOI to a Descent Orbit Insertion (DOI) propagated for 3 days. Overall trajectory contemplated in (a), zoomed in for (b). The illusion of a spiral is presented due to the relative velocity of the Moon around Earth. This illusion allows for a full visualization of the orbit for the 3 days before the descent phase illustrated in green at the end of the orbital trajectory.

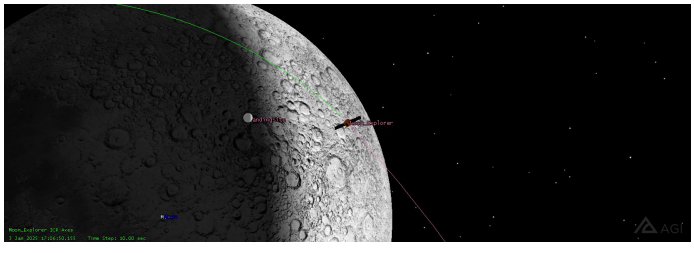

(a) *Lunar Explorer* orbiting around the Moon at the moment of executing the DOI maneuver. The landing site and Moon can be observed underneath the spacecraft.

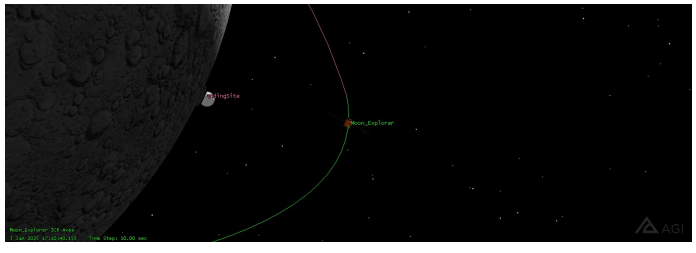

(b) Alternative side view of the *Lunar Explorer* orbiting around the Moon, during the DOI maneuver for a better comprehension of the altitude at the beginning of the descent.

Fig. 11: **STK DOI Maneuver**: View of the *Lunar Explorer* spacecraft when the DOI maneuver takes place.

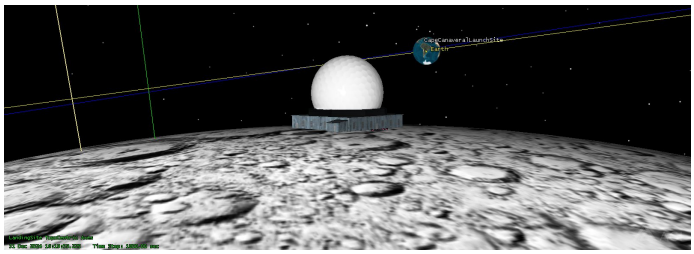

(a) Initial launch from Cape Canaveral. A view of the launch site is exaggerated for visualization purposes.

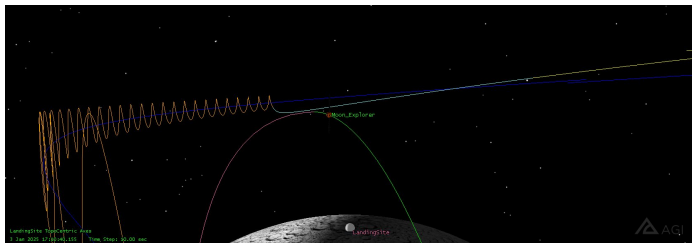

(b) Lunar orbit trajectory observed in orange before beginning descent trajectory.

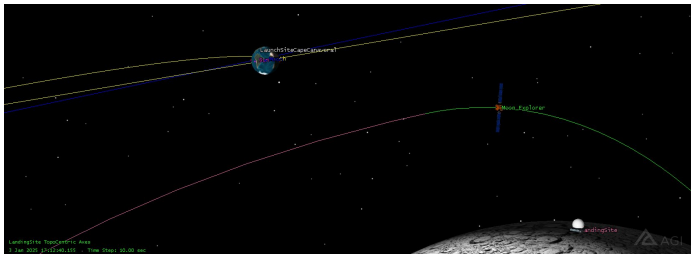

(c) View of the lunar descent with Earth in the background.

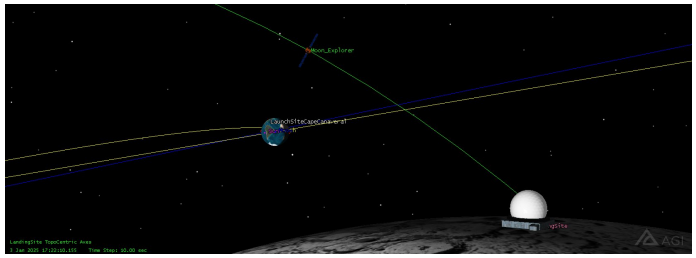

(d) Final approximation of the Ore Retriever and Extraction Rover to the landing site.

Fig. 12: **STK Descent Segment**: In (a), the launch site has been created as a fictitious lunar base solely for decorative purposes. A view of the descent trajectory in sequential order in (b), (c), and (d) is shown. The change from the lunar orbit to the descent phase occurs after the *Descent Orbit Injection* and is differentiated by changing the trajectory color from pink to green. Further observations for the DOI are contemplated in Figure 11

reach the Moon. The ΔV for this trajectory type is detailed in Table V.

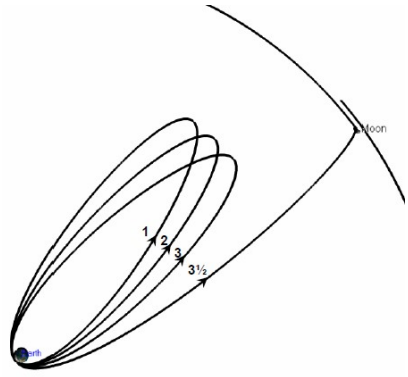

Fig. 13: 3½ Phasing Loop Transfer in Sun- Earth Rotating Coordinates

TABLE V: 3.5 Phasing Loop [10]

Phases	Values
Launch (UTC)	2 Feb 2010 01:44
TOF	22.18 days
TLI ΔV	3,096 m/s
ΔV without descent	873 m/s
Powered Descent ΔV	2,350 m/s
Total ΔV	**6,319 m/s**

B. Weak Stability Boundary (WSB) Transfer

Another method of Lunar transfer is the Weak Stability Boundary (WSB) transfer. The transfer trajectory leaves the Earth with an apogee around $1.5\text{x}10^6 km$, and falls back into Earth orbit, but with a radius of perigee increased by the Sun's perturbations so that it co-orbits the Earth with the Moon. As a result, the spacecraft can enter lunar orbit with no maneuver, although it is a highly unstable orbit, and must be controlled. This is shown in Figure 14 in Sun-Earth rotating coordinates. Although the TLI maneuver for the WSB is greater than for the standard ballistic transfer, there can be a lunar capture ΔV savings of about 25% when capturing into a Lunar orbit. Table VI shows the ΔV values for this trajectory.

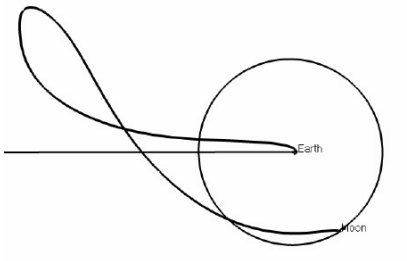

Fig. 14: WSB Transfer in Sun-Earth Rotating Coordinates

TABLE VI: Weak Stability Boundary Transfer [10]

Phases	Values
Launch (UTC)	26 Nov 2009 04:41
TOF	90 days
TLI ΔV	3,194 m/s
ΔV without descent	712 m/s
Powered Descent ΔV	2,331 m/s
Total ΔV	**6,237 m/s**

C. Earth to Earth-Moon L1 to Lunar Orbit Transfer

There have also been proposals and studies of first transferring to a Lissajous orbit at the Earth-Moon L1 point, possibly rendezvousing with a space station there, and then continuing on to Lunar orbit. This is sometimes referred to as an "L1 Gateway" trajectory. This type of trajectory transfer is illustrated in Figure 15 with corresponding ΔV values in Table VII.

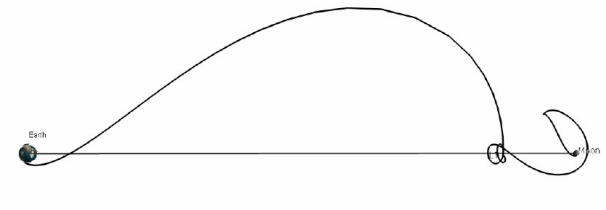

Fig. 15: Earth to L1 to Lunar Landing in Earth-Moon Rotating Coordinates

TABLE VII: Earth to Earth-Moon L1 to Lunar Orbit Transfer [10]

Phases	Values
Launch (UTC)	22 Jan 2010 01:47
TOF	33.2 days
TLI ΔV	3,117 m/s
ΔV without descent	1,566 m/s
Powered Descent ΔV	1,952 m/s
Total ΔV	**6,636 m/s**

D. Justification

The trajectory approach utilized for the mission in consideration, as discussed in subsubsection II-B3 can be compared to the other approaches for this mission. However, in order to do that, the comparison should be made for comparative launch windows. The data for the chosen ballistic transfer trajectory, but in the same time window as other options, is shown in Table VIII.

The comparison for the total ΔV requirements corresponding to each trajectory approach is displayed in Table IX.

Therefore it can be justified that the chosen ballistic trajectory approach not only takes the minimum amount of time to reach the lunar orbit, but also the minimum amount of ΔV, therefore requiring the least amount of fuel for the spacecraft of the same specifications.

TABLE VIII: 5-Day Ballistic Transfer to Lunar Orbit [10]

Phases	Values
Launch (UTC)	19 Feb 2010 00:23 UTC
TOF	5.23 days
TLI ΔV	3,137 m/s
ΔV without descent	845 m/s
Powered Descent ΔV	1,915 m/s
Total ΔV	**5,897 m/s**

TABLE IX: ΔV comparison for different trajectories

Approach	ΔV as %
5-Day to Lunar Orbit	100%
3.5 Phasing Loop	107%
WSB	106%
L1	113%

It can also be seen that the duration of the ballistic trajectory depends on the launch windows. For the reference taken in this section, it gives the minimum ΔV for a transfer of 5 days. However, for the chosen launch date of the mission in consideration, it is achieved in 4 days, as mentioned in subsubsection II-B3

IV. Mission Analysis & Design

A. Landing Site

The selection of landing site near the lunar north pole is based on the following considerations.

1) **Accessibility and Landing Site Selection:** The lunar poles offer relatively accessible locations for landing spacecraft and conducting surface operations. The terrain near the poles tends to be flatter compared to other regions of the Moon, reducing the complexity and risk of landing missions. Accessible landing sites near the lunar north pole enable easier deployment of mining equipment, robotic systems, and scientific instruments, facilitating technology demonstration activities and data collection. And thereby reducing logistical challenges and mission complexity.
2) **Water Ice Deposits:** The lunar north pole is known to contain permanently shadowed regions (PSRs) where temperatures are extremely cold and stable, possibly preserving water ice deposits. These PSRs are believed to have accumulated water ice from comet impacts and possibly from solar wind interactions with the lunar surface. Water ice is a critical resource for future space exploration, as it can be used for drinking water, oxygen production, and most importantly, as a source of hydrogen and oxygen for rocket propellant. Demonstrating the ability to extract water ice from the lunar north pole could pave the way for sustained human presence and exploration beyond low Earth orbit.
3) **Solar Power Availability:** While certain areas near the lunar poles experience long periods of darkness due to the orientation of the Moon's axis, there are also regions that receive near-continuous sunlight. These

areas, located near the poles' periphery, offer the potential for solar power generation to support mining operations. Solar power can be harnessed to provide energy for mining equipment, processing facilities, and other infrastructure.

4) **Scientific Interest and Resource Potential:** In addition to water ice, the lunar regolith near the poles may contain other valuable resources such as helium-3, rare earth elements, and other volatiles. Mining technology demonstration missions to the lunar north pole provide an opportunity to explore and characterize these resources, advancing our understanding of lunar geology and resource potential. Scientific investigations conducted as part of these missions can contribute valuable data and insights into lunar evolution, planetary science, and the formation of the solar system.

TABLE X: Landing Site Location

Parameter	Value
Latitude	82.485° North
Longitude	132.309° West
Elevation	0

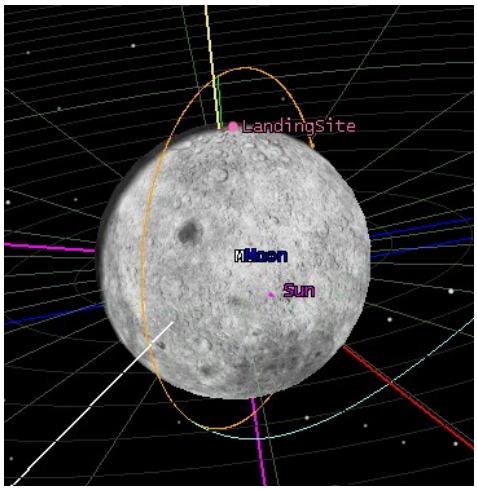

Fig. 16: Landing Site found in the northernmost region of the Moon, where ice concentration has been found the highest.

B. Mining Strategy

In the pursuit of resource utilization beyond Earth, humanity stands at a pivotal juncture. An ever-growing demand for rare minerals and the necessity for sustainable practices is pushing humanity towards the exploration of celestial bodies. In this case, the Moon presents an unparalleled opportunity. The Moon acts as an analogous example of what we can expect from comets. Comets are icy remnants from the early stages of our solar system, and harbor a wealth of resources crucial for scientific research and future space endeavors. However, accessing these resources in the demanding and chaotic environment of space poses formidable challenges.

Comets and asteroids entail low, irregular gravitational environments, abrasive dust particle cloud propagation, high exposure to radiation, and enormous differences in luminosity due to the rotational velocities of these Solar System Small Bodies (*SSSB*s). These environmental effects are a constraint to the strategy to follow in sample collection.

To address these challenges, the mission embarks in the footsteps of other pioneers, and harnesses the state-of-the-art developments in robotics and advanced mining technology. At the forefront of our payload strategy is the Regolith Advanced Surface Systems Operations Robot (*RASSOR*), a versatile and highly efficient mining robot specifically designed for extraterrestrial exploration in low gravitational environments. *RASSOR* represents the culmination of years of research and development, embodying the ingenuity and innovation essential for space exploration in the 21st century. [12], [13].

RASSOR Physical Properties

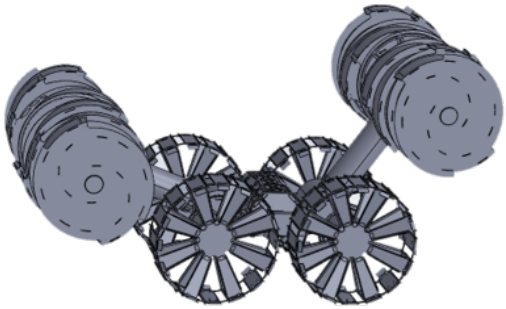

Fig. 17: RASSOR: Regolith Advanced Surface Systems Operations Robot.

The RASSOR appears to be a suitable method for mining for several reasons:

- **Adaptability:** RASSOR is designed to operate in an extraterrestrial environment, specifically on the Moon. Its tank tread mobility system allows it to navigate and excavate in lunar regolith effectively.
- **Excavation Efficiency:** The dual counter-rotating bucket drum design of RASSOR minimizes excavation forces, allowing it to collect and transport regolith efficiently. This design helps in reducing the reaction forces on the robot, making it suitable for low-gravity environments.
- **Mining Depth Capability:** RASSOR is equipped to mine both the top 5 cm of surface regolith for nominal operations and up to 1 meter deep for icy regolith mining. This flexibility allows it to access different layers of the lunar surface.
- **Remote Operation:** RASSOR can be controlled remotely using a driver station software on a laptop, enabling operators to oversee and control mining operations from a safe distance.

- **Self-Righting Capability:** The ability of RASSOR to self-right itself using its dual arm configuration adds to its robustness, especially in challenging lunar terrain.
- **Mission Duration and Recharging:** With a five-year mission duration, RASSOR is designed to operate for an extended period. It uses rechargeable batteries that can be replenished at the lander between mining treks, ensuring sustained operations.
- **Cameras for Monitoring:** Equipped with one or more cameras, RASSOR provides visual monitoring of its operations, aiding in real-time decision-making and control.

TABLE XI: Key Technical Parameters of RASSOR

Parameter	Value	Unit
Power Source	Li-ion Battery	-
Battery Capacity	1,410	Whr
Max Driving Slope	20	°
Max Obstacle Height	75	cm
Regolith Delivered per Trip	90	kg
Max Speed	49	cm/s
Trips per Charge (100m)	20	Trips
Dry Mass	67	kg
Energy per Delivered Regolith	0.761	Whr/kg

1) Moon Chemical Composition: The lunar surface consists of a mixture of ice and other volatile materials. For analysis, the lunar regolith is assumed to have an average chemical composition, to help us understand what can be sampled and to identify regions of interest. [3], [14].

Table XII shows the chemical composition that is to be expected [15], [6], [4].

Where the methods used are:

- R: Spectroscopy
- IR: Infrared Spectroscopy
- MS: Mass Spectrometry
- UV: Ultraviolet Spectroscopy
- V: Visible Spectroscopy

And the origin are:

- P: Proximal. Indicates that the measurement or observation is made from a proximal location.
- D: Distal. Indicates that the measurement or observation is made from a distal location, often from a distance, such as Earth-based observations or telescopic measurements.

As it can be noted from Table XII, ice is abundant in the lunar regolith. Knowing that the approximate weight percentage of H_2O is 80%, means that 80% of the total mass available in the Moon is composed of H_2O molecules.

2) Example Use Case: An example use case of how the mined resources can be utilized, is to provide oxygen to the ISS crew. In this example, it is calculated how much regolith should be extracted to convert the ice into sufficient oxygen for an assumed ISS crew of 6. This is the average crew year-round, for a year [24].

To extract the H_2O molecules from the ice, the regolith sample is to be collected. Due to the presence of other volatiles, the sample must be purified. In this case, the purification method followed where water is extracted is the *Pressure Swing Adsorption (PSA)* method. In *PSA*, the gas mixture is passed through an adsorbent material under high pressure. The adsorbent selectively retains certain gases while allowing H_2 and/or O_2 to pass through. The pressure is then reduced to release the purified gas. Some advantages of *PSA* are its simplicity, compactness, and no requirement of cryogenics. It is relatively simple and can operate cyclically, is originally designed to be compact and lightweight, and operates at ambient pressures, avoiding the need for cryogenic systems.

Then, the process of Proton Exchange Membrane (*PEM*) electrolysis can be employed. In *PEM electrolysis*, an electric current is passed through water (H_2O) in an electrolysis cell equipped with a proton exchange membrane. This membrane separates the two electrodes and allows only protons ($H+$) to pass through while blocking the passage of gas and liquid. When the electric current is applied, water molecules near the anode undergo oxidation, releasing oxygen gas (O_2) and positively charged hydrogen ions ($H+$). Meanwhile, at the cathode, hydrogen ions gain electrons and form hydrogen gas (H_2). The PEM separates the oxygen and hydrogen gases produced during electrolysis, allowing them to be collected separately.

Limitations of *PEM electrolysis* include its dependency on a reliable source of electricity, which may be challenging in remote locations such as comets. Additionally, high efficiency is required to ensure the economic feasibility of large-scale oxygen production using *PEM electrolysis*.

However, *PEM electrolysis* offers several advantages over other methods. It is a clean and environmentally friendly process, as it does not produce any greenhouse gases or other harmful emissions. It can also be operated at relatively low temperatures and pressures compared to other electrolysis methods, reducing energy requirements and equipment costs. Furthermore, the use of a proton exchange membrane allows for the selective separation of oxygen and hydrogen gases, resulting in high purity oxygen production.

Additionally, the extracted hydrogen as a byproduct, can be used for various purposes, including as a propellant for rockets, for metal reduction processes, or for power generation in fuel cells.

In summary, these are the steps that involve the extraction and purification of oxygen:

TABLE XII: Components in Approximate Weight Percentage, Method of Analysis, Origin, and Mixing Ratio Range expected to be found in Lunar Regolith

Component	Approx. Weight %	Method	Origin	Mixing Ratio Range (M.R.%)
Water (H_2O)	80	R, IR, MS	P	100
OH	-	R, IR, UV	D	100
CO	Varies	R, IR, UV, MS	P, D	0.4 – 30
CO_2	Varies (0.01% to 20%)	IR, MS	P	2 – 6
CH_4 (Methane)	Varies	IR	P	0.14 – 1.4
C_2H_2	Varies	IR, MS	P	0.2 – 0.5
C_2H_6	Varies	IR, MS	P	0.11 – 0.67
CH_3OH (Methanol)	Varies	R, IR, MS	P	1 – 7
H_2CO	Varies	R, IR	P	0.2 – 0.6
NH_3 (Ammonia)	Varies	R, IR, MS	P	0.5 – 1.5
HCN	Varies	R, IR, MS	P	0.02 – 0.15
NH	Varies	V	D	0.11 – 1.6
S_2	-	UV	?	0.0012 – 0.005
SO_2	-	R	P	0.2
SO	-	R	D	0.2
H_2S (Hydrogen Sulfide)	Varies	R, MS	P	0.2 – 1

1) **Regolith Extraction**: Collect regolith samples from the lunar surface, which contain ice and various volatiles.
2) **Pressure Swing Adsorption (PSA)**: Purify the regolith samples using the PSA method.
   - Pass the regolith sample through an adsorbent material under high pressure.
   - Selectively retain certain gases while allowing H_2 and/or O_2 to pass through.
   - Reduce the pressure to release the purified gas, containing water vapor and other volatile compounds.
3) **Proton Exchange Membrane (PEM) Electrolysis**: Perform PEM electrolysis on the purified gas to extract oxygen.
   - Set up an electrolysis cell with a proton exchange membrane.
   - Pass an electric current through the purified gas in the electrolysis cell.
   - Allow water molecules to undergo electrolysis, separating into oxygen gas (O_2) and hydrogen gas (H_2).
   - Collect the oxygen gas produced at the anode side of the electrolysis cell.

3) Use Case Calculations: All processes previously mentioned are not perfect. Therefore, efficiencies have to be taken into account. Table XIII describes the practical efficiencies encountered from practical results in real mining processes.

TABLE XIII: Efficiencies of all Processes Involved

Parameter	Value
Recovery rate of the PSA process	60%
Oxygen purity	98%
Weight content of water within lunar sample	80%
PEM Electrolysis efficiency	80%

Using the data compiled in Table XI and Table XIII, the mass requirements of the regolith at each step of the involved process for the specific use case, can be calculated and are found in Table XIV and Table XV for the regolith mass and RASSOR mission plan, respectively.

TABLE XIV: Calculations of Masses and Trips Required for Theoretical Use Case

Parameter	Value	Unit
O_2 Consumption per person per day	0.84	kg/pax/days
Total ISS O_2 Consumption	1,840.86	kg
H_2O Required for Electrolysis	4,141.96	kg
H_2O to be Purified through PSA	5,177.45	kg
Total Regolith to be passed through PSA	8,805.20	kg
Total Regolith Mass required	11,006.49	kg
Total Time for 1 trip	3.7	hours
# Trips required	138	-
Total Time Sampling	21.25	days

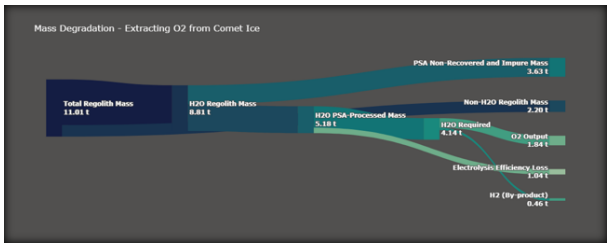

Fig. 18: Mass Degradation through O_2 extraction process from original regolith collected by RASSOR.

TABLE XV: RASSOR Requirements and Mission Information

Parameter	Value	Unit
Total Power Consumption	8,375.94	Whr
# of Batteries	6	-
Total Distance Travelled	27.6	km
Total Time Sampling	21.25	days
Current TRL	4	-
Expected TRL by 2029	6	-

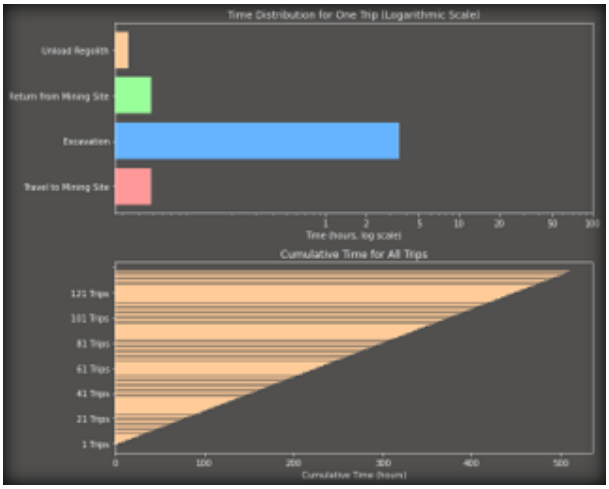

Fig. 19: Individual time required per RASSOR activity, and overall mining time.

V. Spacecraft System Design

A. Communication System

The communication system is used to communicate with Earth as well as between modules. Within this system, there are two main data groups: the TT&C (telemetry, tracking, and command) and the science data. Both are equally important and deserve to be looked at individually.

1) Science data:

Science data is all the data collected by the payload during the mission from measurements and observations. This information is not essential to the mission itself. It is only transmitted by the spacecraft to Earth (downlink) and usually requires the highest data rates in the communication system.

For this link, the Ka-band was chosen because it is the highest frequency band used for satellite communication, allowing for the greatest bit rate, which is attractive for science data links. The more data one can transmit the more valuable the mission becomes. However, this band has some drawbacks, such as its high susceptibility to atmospheric conditions and, since it uses high frequencies, it also requires high transmitting power and/or high gain antennas to maintain error-free communication. The exact frequency selected was $f = 31,8$ GHz as this is within the allowed range from ITU [2], and is the frequency used by the selected ground stations network, DSN [21].

Regarding the COTS hardware, the following components were selected:

- **HRT150 by General Dynamics:** it was the only Ka-band transmitter found on the market.
- **Beamsat Horn Antenna by Picosats:** highest-gain Ka-band antenna found on the market.

2) TT&C:

This part of the communication system aims to transmit information about the health and status of each subsystem, as well as the position and orientation of the spacecraft. It is also used for remote control if required.

The chosen frequency band was the X-band as it is the highest frequency band that is immune to atmospheric effects, allowing for atmosphere-independent communication. This is especially important for TT&C as it is mission-critical information. The exact frequencies selected are $f = 7,145$ GHz for uplink and $f = 8,4$ GHz for downlink. Again these were chosen based on allowed ranges [2] and DSN availability [21].

Four links are established during mission operation:

- Earth - Main Module (Uplink)
- Main Module - Earth (Downlink)
- Main Module - Ore Retriever (Downlink)
- Ore Retriever - Main Module (Uplink)

For these links, all the components are COTS:

- **SDST by General Dynamics:** a TRL9 transponder used for communicating with Earth, both uplink and downlink. It requires low power but has a high enough transmitting bit rate for the low requirements for TT&C.
- **XLINK-X by IQ Spacecom:** a TRL9 transceiver that will be integrated both in the Main Module and the Ore Retriever, designed for CubeSats but easily adaptable for the links between the two modules.
- **X Band Antenna by IQ Spacecom:** a TRL9 4-patch antenna capable of receiving and transmitting at the same time. Again one is used in each module for the links between them.
- **Beamsat Horn Antenna by Picosats:** the same horn antenna used for the Ka-band link will be used to transmit and receive in the X-band.

B. ADCS

1) Sensors:

The combination of sensors has been carefully selected out of those available, based on the accuracy requirements of the mission to be within 0.05 degrees. This is one of the reasons why both the sun sensors and the star trackers have been chosen to overcome their drawbacks, as well as offer a combined high level pointing accuracy, especially during the launch. As shown in Table XVI, while the star trackers offer a much higher degree of accuracy, they are not very effective under direct sunlight, which is when the attitude determination is primarily dependent on the sun sensors. The choice of the gyroscope has been dictated by the gyro angular random walk, which is the measure of accuracy and lower noise characteristics, as well as the fact that it offers 4-axes tetrahedral redundancy. The overall combination of sensors offers multiple redundancies so as not to hinder the success of the mission if any of them go faulty.

TABLE XVI: Sensors and their standout performance parameters

Sensors	Parameters	Values
Gyroscope [20] - (1x4)	ARW	0.0002°/hr
	Range	±35°
	Power	40 W
	Mass	8 kg
Sun Sensor [19] - (5)	Accuracy	<0.02°
	FOV	128°
	Power	1 W
	Mass	0.33 kg
Star Tracker [16] - (3x2)	Accuracy	<0.001°
	FOV	20°
	Power	8.9 W
	Mass	3.55 kg

TABLE XVII: Actuators and their standout performance parameters

Actuators	Parameters	Values
Thrusters (12)	Max Thrust	22 N
	Fuel	Hydrazine
	Oxidizer	Nitrous Oxide
CMG [17] - (1x4)	Torque	60 Nm
	Momentum	30-45 Nms
	Power	30 W
	Mass	38 kg

2) Actuators:

For the satellite in consideration, it can be fairly easily deduced that momentum exchange devices are very much incompetent given their actuation limit, and therefore a very frequent need to be desaturated by thrusters. Hence, thrusters are chosen as primary actuators for major attitude correction, leaving the final precision to CMGs, which are in accordance with the simulation results, and have enough capacity to maintain pointing accuracy.

Choice of Thruster

For the choice of the thruster, it was chosen to be bi-propellant, the same as the main propulsion system to share the mutual fuel reservoirs and avoid the dead weight of carrying extra structural mass. They are also preferred over other types for the following reasons:

- **Electrical Thrusters** are extremely power consuming, more or less 90% is devoted simply to keep it ready to use and only 10% is due to the thrust produced, therefore electric propulsion units are often coupled with extremely large solar panels.
- **Cold-Gas Thrusters** use a non-reactive gas, stored at high pressure (around 30 MPa), commonly use Nitrogen SP 70s or Helium SP 175s. Helium saves mass but is more prone to leakage and more expensive, not to mention the extra structural mass of tanks.

The configuration used is typical for a thruster attitude system, and involves 12 units arranged in the lower part of the satellite as shown in Figure 20 so that the rotations around the three axes are controlled by 4 thrusters each, thus offering redundancy.

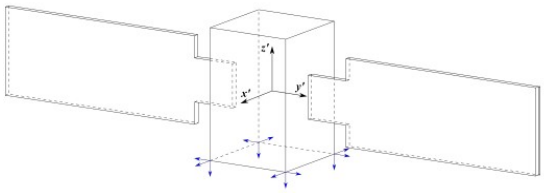

Fig. 20: Arbitrary satellite showing thruster configuration

C. On-Board Computers & Software

The On-Board Computing System (OBCS) selected for the mission has the specifications as shown in Table XVIII. This particular subsystem embodies hardware components meticulously tailored to the needs of extraterrestrial exploration. Anchored by a robust Intel Movidius Myriad X Vision Processing Unit and complemented by the Unibap COMexpress e23 family processing core, the system has processing power critical for real-time data analysis and decision-making. Dual Ethernet ports with 10 GbE (10GBASE-T) capability ensure high-speed communication between the satellite and ground station, facilitating seamless command and control operations. This is illustrated as a use case example in Figure 21 Additionally, the inclusion of FPGA DSP cores and OpenCL/HIP GPU accelerators empowers the system to handle complex signal processing tasks and parallel computing challenges inherent in surface observation and mining operations.

TABLE XVIII: On-Board Computer Specifications: SpaceCloud iX10-101A

Parameters	Values
RAM	24 GB DDR4 ECC (CPU/GPU)
Storage	1 x 3.8 TB NVMe SSD 1 x 128 GB SATA SSD
Mass	<900 grams
Power	<40 W
Operating System & Software	SpaceCloud OS (Linux)

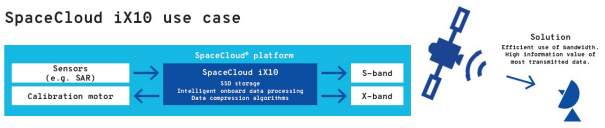

Fig. 21: Use Case Example of the selected on-board computer

D. Structural Design

A CAD of the whole spacecraft was modeled using *SOLIDWORKS*, where each subsystem was strategically placed taking into account the thermal and ADCS

requirements. Systems that require low temperatures for correct operation like the TT&C and OBCS systems, as well as the cameras, were separated as much as possible from heat sources, like batteries. Symmetry was maintained as much as possible throughout the design to aim for a central of gravity close to the centroid of the satellite. All components of each system were kept together to reduce cable length and transportation losses. Finally, the mission concept of operations was also considered when choosing sensor placement.

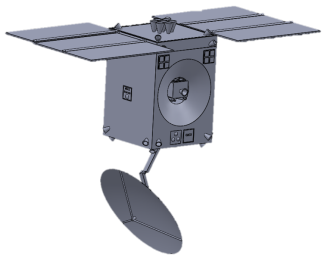

Fig. 22: Main module deployed.

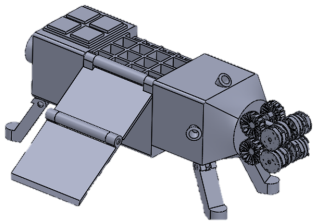

Fig. 23: Ore retriever deployed.

1) Mass and Volume Budget:

With all the components defined it was possible to do a complete mass budget. For components whose mass could be found, an estimate was made based on other missions. Table XIX summarizes the results.

The volume of the spacecraft was derived from the maximum allowed by Starship [1], using cuboids instead of spheroids due to the practicality of having flat faces for component placement and integration. The resulting total volume can be seen in Table XX.

E. Propulsion Subsystem

The selection of a propulsion system for the mission involves a comprehensive analysis of available options. Trade-offs were made to evaluate different propulsion systems, including electrical propulsion.

For electrical propulsion, initial considerations were made for its use as the main engine and secondary propulsion system. However, challenges such as the time required to achieve orbits and operational costs led to the dismissal of this option. The study included potential thrusters like the Ariane Group RIT 2X ion thruster and Aerojet Rocketdyne AEPS hall thruster.

Another aspect considered was the selection of propellants for the propulsion subsystem. Criteria such as propulsion system mass, volume, material compatibility, hazards, storability, ignition, combustion, cost, and technological readiness were evaluated as proposed by [22] and [7]. Three bipropellant options were considered: MMH/NTO, Ethanol/H_2O_2, and Propylene/N_2O. These are found in Table XXI.

The first trade-off involved grading each propellant combination based on established criteria and weights and is found in Table XXI, Table XXII and Table XXIII. MMH/NTO emerged as the most suitable option, considering factors like mass, volume, compatibility, hazards, storability, ignition,

TABLE XIX: Mass Budget

Subsystem	Component	Quantity	Total Mass [kg]
Propulsion	Main Thrusters	7	31.71
	Propellant Tanks	4	340.46
	Pressuring Tanks	2	49.32
	Lines and Valves	1	9.06
ADCS	Gyroscope	1	8.00
	CMG	4	38
	Sun sensors	5	1.65
	Star trackers	3	3.55
	Attitude Thrusters	24	10.90
Power	Solar Arrays	2	115.40
	Solar Array Drive	2	4.60
	Power Control Unit	1	4.05
	Wiring	1	180,00
	Battery	1	33.00
Thermal	Radioisotope heater	100	3.40
	MLI	1	0.50
OBCS	SpaceCloud Computer	2	1.80
Structure	Main Module	1	393.08
Payload	Camera	1	1.00
	LIDAR	1	7.00
	IR camera	1	4.46
	RASSOR	1	67.00
	Ore Retriever	1	258.62
TT&C	Reflector	1	4.97
	Ka Antenna	1	0.57
	X Antenna	1	0.02
	X Transceiver	1	0.20
	X Transponder	1	3.20
	Ka Transmitter	1	2.27
Total Dry Mass			1,378
Propellant Mass			13,300
Total Wet Mass			14,678
Observation Module			6,000
Total Mass			20,678

TABLE XX: Simplified Volume Budget

Module	Shape	Volume [m^3]
Main Module	parallelepiped	256
Observation Module	frustum of a square pyramid	163
Total		419

cost, and technological readiness.

TABLE XXI: Types of propellant

	MMH/NTO	Ethanol/H_2O_2	Propylene/N_20
ρ_{ox} [kg/m^3]	1,448	1,390[1]	1,220[2]
ρ_{fu} [kg/m^3]	878	789	611[2]

[1]At 20°C. [2]At the boiling temperature.

TABLE XXII: Criteria and Weights

Criteria	Weight [%]
Propulsion System Total Mass	25
Propulsion System Volume	20
Material Compatibility	12,5
Hazards	10
Storability	12,5
Ignition & Combustion	10
Cost	10
Technological Readiness	20

TABLE XXIII: First trade-off results.

Criteria	MMH/NTO	Ethanol/H2O2	Propene/N2O
Pro. sys. mass	3	3	2
Pro. sys. volume	3	2	1
Mat. compatibility	2	1	2
Hazards	1	3	3
Storability	3	2	1
Ignition	3	2	1
Cost	1	2	3
TRL	3	2	2
Final Grade	3.075	2.625	2.175

In the second trade-off, as provided in Table XXIV, different COTS main engine/thruster combinations using hydrazine-based propellants were evaluated. A high thrust MMH/NTO R-42 from Aerojet Rocketdyne / R-6D from Aerojet Rocketdyne, featuring a high-thrust MMH/NTO propellant combination, was selected as the winner based on criteria such as propulsion system mass, volume, tank similarity, heritage, and reliability. Consult Table XXIV and Table XXV.

TABLE XXIV: Criteria and Weights

Criteria	Weight [%]
Propulsion System Total Mass	25
Propellant Volume	20
Tank Similarity	10
Heritage	25
Reliability	20

Finally, the total required propellant mass and volume were computed using the Tsiolkovsky equation, considering the maximum allowed wet mass and ΔV requirements. The chosen propellant combination required 13.3 tons of total mass and 11.44 m³ of volume.

F. Power System

The spacecraft's power subsystem plays a critical role in ensuring the success of the mission by providing the required power to all onboard systems. It is responsible for generating, storing, and distributing electrical energy throughout the spacecraft. Due to the harsh environment of space, where sunlight, temperature variations, and radiation can pose significant challenges. Thus, the design and operation of the power subsystem must be carefully engineered to meet the mission objectives, while ensuring reliability and longevity.

TABLE XXV: Second trade-off results.

Configurations	1	2	3	4	5	6
Prop. sys. mass	5	6	3	4	2	1
Prop. volume	5	6	3	4	2	1
Tank similarity	6	6	6	6	5	4
Heritage	4	5	5	3	6	5
Reliability	3	6	3	6	3	3
Total	4.35	5.75	3.6	4.35	3.15	2.7

TABLE XXVI: Total propellant required.

Propellant	Mass [t]	Volume [m^3]
Oxidizer	8.269	5.73
Fuel	5.034	5.71
Total	13.3	11.44

1) Power Budget:

The power budget includes all the power requirements by the different subsystems onboard. It is a crucial aspect, as a careful estimation and management of power consumption will ensure sufficient energy is available in the different cases the spacecraft will encounter throughout the mission.

In this case, the vast amount of the mission will be spent traveling to the Moon. Additionally, the orbit around the moon has a great inclination. This infers that eclipses are not a concern. Additional calculations on eclipse times shall be considered in later stages of the mission planning. For now, a system margin of 10% is considered a conservative approach due to uncertainties and the mission being in its early stages. Table XXVII collects all values for each subsystem and subcomponent of each respectively.

TABLE XXVII: Power Budget

Subsystem	Component	Power (W)
ADCS	Gyroscope	25
	CMG	30
	Sun sensors x 5	1
	Star trackers x 3	8.9
Power	Solar Array Drive Assembly	0.5
	Power Control Unit	1.25
OBCS		7
Payload	Camera	0.9
	LIDAR	40
	IR camera	9.9
	RASSOR	16.42
TT&C	X Transceiver	16
	X Transponder	15.8
	Ka Transmitter	47
Total Power Requirement		219.67
System Margin (SM)		10%
Total Power Requirement with SM		239.67

2) Trade-Off & Requirements:

Typically, there are four types of power sources for spacecraft. *Photovoltaic* solar cells, which are the most common source, convert incident solar radiation directly to electrical energy. *Static power* sources use a heat source, typically plutonium-238 or uranium-235 (nuclear reactor), for direct thermal-to-electric conversion. *Dynamic* power sources also use a heator source, typically concentrated solar radiation, plutonum-238, or enriched uranium. These sources convert power using the Brayton, Stirling, or Rankine cycles. The last power source is the *fuel cell*, which is normally used on manned space missions.

Due to volume constraints, technology, fuel availability, and reliability, a *solar photovoltaic* is chosen as the power source. In comparison, solar cells are cheaper and non-hazardous in comparison to radioisotopes [9].

3) Solar Arrays:

The process of determining solar array specifications for the mission involves several steps:

1) Determine requirements and constraints for power subsystem solar array design.
2) Calculate the amount of power to be produced by the solar arrays.
3) Select the type of solar cell and estimate power output.
4) Determine the beginning-of-life (BOL) power production capability per unit area of the array.
5) Determine the end-of-life (EOL) power production capability for the solar array.
6) Estimate the solar array area required.
7) Estimate the mass of the solar array.

In the design, a trade-off between mass, area, cost, and risk must be considered. **Gallium arsenide** cells are chosen over silicon due to their advantages despite being costlier. The solar array area required is estimated using equations considering factors like sunlight flux, array efficiency, and packing factor. The beginning-of-life (BOL) and end-of-life (EOL) power production capabilities are calculated considering inherent degradation and mission duration.

The solar array area required for the spacecraft is determined to be $84m^2$. However, solar array sizing is complex due to variations in geometry and angle of incidence, necessitating constant determination or worst-case angle calculations for accurate estimation of end-of-life power production.

4) Battery:

For energy storage in the spacecraft, a secondary battery, specifically a Lithium-ion battery, is selected due to several advantages over traditional battery types like Nickel-Cadmium (NiCd) and Nickel-Hydrogen (NiH_2). Lithium-ion technology offers higher energy density and a wider operating temperature range compared to NiCd and NiH_2 batteries. The nominal operating voltage of Lithium-ion cells allows for a reduction in the number of cells required, resulting in reduced mass and volume for aerospace applications. Lithium-ion batteries also provide significant volume and mass advantages over traditional counterparts.

Key constituents of Lithium-ion batteries contribute to their higher energy density and wider operating temperature range. These batteries are under development, offering specific energy densities ranging from 70 to 110 Wh/kg, making them promising for aerospace applications where higher energy densities are desirable.

The required battery's operational capacity can be calculated according to Equation 1 by using the required power during eclipse $P_{Eclipse}$, eclipse duration $t_{Eclipse}$ and the depth of discharge, DOD, of the battery.

$$C_{bat} = \frac{P_E t_E}{60 \times 60} \frac{100}{DOD} \tag{1}$$

5) Final Characteristics:

To comply with the power requirement, two deployable solar array wings manufactured by *DHV* are selected [5]. The arrays fulfill the power requirements and each wing deploys to 3 panels, each with a dimension of $1,000 \times 3,039mm$. Additionally, and as previously mentioned, calculating the real power requirement is more complex than applying a set of theoretical equations, even if values obtained through practical experimentation are used for variables such as efficiencies. Therefore, the solar array dimensioning and capabilities must take into account a margin, to compensate for. The rest of the relevant characteristics of the solar arrays are collected in Table XXVIII.

For the battery selection, the COTS option shall be Li-ion, shall survive for at least the mission lifetime, which corresponds to $27,000$ cycles, and shall have the minimum capacity of $966.7Wh$. Therefore, a *ibeos B28-1100 Satellite Battery* is selected [18]. The rest of the relevant characteristics of the battery are collected in Table XXVIII.

TABLE XXVIII: Final Battery & Solar Array Characteristics

Component	Property	Value	Unit	Solution Values
Battery	Operational Capacity	966.7	Wh	1,100
	DOD	30	%	30
	Lifespan	27,000	Cycles	40,000
	Battery Type	Li-ion	-	Li-ion
Solar Array	Power BOL	488.92	W	1000
	Power EOL	437.45	W	-
	Degradation	-2.75	%/year	-
	Area	84	m^2	2x(3x7.5x2) = 135
	Incidence Angle	0	°	-

G. Thermal Control

In spacecraft design, thermal control is crucial to ensure that all instruments operate within their temperature ranges

effectively.

The spacecraft system simplifies the thermal considerations, with the main body serving as a significant component with thermal inertia, to which critical instruments are attached. These instruments include the on-board computer system and two cameras, modeled to influence the main body's temperature through heat flow via thermal conduction and structural connections.

Environmental effects, such as day-night cycles and solar radiation, are simulated to anticipate worst-case scenarios, including eclipses. The simulation accounts for the oscillatory nature of solar radiation, mimicking the dimming effect as the sun rises and sets. Additionally, radiation losses are considered.

The output reveals that the spacecraft's temperature remains within its operational range. The plot demonstrates nonlinear temperature fluctuations during thermal cycles, notably a decrease when the sun is occluded and a subsequent increase upon solar exposure. The peaks of temperature decrease progressively with each night-day cycle, indicating system stabilization toward equilibrium.

To maintain thermal stability, two solutions are implemented: an active approach employing a 7W electric heater during cold phases to raise critical component temperatures, and a passive approach utilizing multi-layer mylar insulation to reduce temperature fluctuations and losses in the system.

VI. Conclusion

The advent of SpaceX's Starship presents a compelling opportunity to revolutionize space missions by significantly reducing costs and expanding the realm of feasible exploration endeavors. The platform's cost-effectiveness enables ambitious missions that were previously considered financially prohibitive to become viable options within the current market landscape.

With the overarching objective of conducting a mining mission to the Main Belt Comets, the decision to send a testing mission to the Moon utilizing the same spacecraft serves a dual purpose. It facilitates comprehensive testing of all subsystems and mining equipment in a nearby and accessible environment, mitigating risks associated with embarking directly on a deep space mission to the comet. Moreover, conducting mining activities on the Moon yields invaluable insights into the feasibility and efficacy of resource extraction techniques, particularly concerning water ice and volatile materials. Confidence in the spacecraft's compatibility with a mining mission to the Main Belt comet is bolstered through lunar testing, laying a solid foundation for future deep space exploration endeavors while capitalizing on the benefits of lunar resource utilization.

In conclusion, the testing mission to the Moon promises to yield invaluable insights and validations for the spacecraft designed for the Main Belt comet mining mission. Meticulous trajectory planning, operational simulations, and subsystem testing in a lunar environment will ascertain the spacecraft's capabilities. Thorough evaluation of subsystem functionality, mining equipment performance, and resource extraction techniques will enhance confidence in the spacecraft's readiness for deep space exploration.

Furthermore, the mission highlights the significance of lunar resource utilization as a precursor to future space missions, offering the potential for extracting Oxygen and Hydrogen fuel to sustainably power space exploration endeavors. The knowledge and experience gained from this testing mission will serve as a robust foundation for the success of the Main Belt comet mining mission, advancing both scientific understanding and practical applications in space exploration.

REFERENCES

[1] Starship users guide, Mar 2020.

[2] ITU Radiocommunication Assembly. Preferred frequency bands for deep-space research in the 1-40 ghz range. *ITU RECOMMENDATIONS*, Rec. ITU-R SA.1012.

[3] Nicolas Biver, Dominique Bockelée-Morvan, Jacques Crovisier, Pierre Colom, Florence Henry, Raphaël Moreno, Gabriel Paubert, Didier Despois, and Dariusz C Lis. Chemical composition diversity among 24 comets observed at radio wavelengths. *Earth, Moon, and Planets*, 90:323–333, 2002.

[4] D Bockelée-Morvan and N Biver. The composition of cometary ices. *Philosophical Transactions of the Royal Society A: Mathematical, Physical and Engineering Sciences*, 375(2097):20160252, 2017.

[5] DHV Technology. Dhv technology products. Accessed: February 14, 2024.

[6] Gianrico Filacchione, Olivier Groussin, Clémence Herny, David Kappel, Stefano Mottola, Nilda Oklay, Antoine Pommerol, Ian Wright, Zurine Yoldi, Mauro Ciarniello, et al. Comet 67p/cg nucleus composition and comparison to other comets. *Space science reviews*, 215:1–46, 2019.

[7] O. Frota, B. Mellor, and M. Ford. Proposed Selection Criteria for Next Generation Liquid Propellants. In A. Wilson, editor, *ESA Special Publication*, volume 557 of *ESA Special Publication*, page 6.1, October 2004.

[8] Joey Klender. Spacex has aggressive plan for starship in 2024 with more than nine launches, Year of publication (if available). Accessed: February 29, 2024.

[9] Wiley J Larson and James R Wertz. Space mission analysis and design. *Torrance, CA (United States)*, 2004.

[10] Timothy Carrico Chuck Deiterich Mike Loucks, John Carrico. A comparison of lunar landing trajectory strategies using numerical simulations.

[11] Exploring Your Mind. The paradox of the ouroboros and the eternal return. https://exploringyourmind.com/the-paradox-of-the-ouroboros-and-the-eternal-return/, Accessed: 2024-02-23.

[12] Robert P Mueller, Rachel E Cox, Tom Ebert, Jonathan D Smith, Jason M Schuler, and Andrew J Nick. Regolith advanced surface systems operations robot (rassor). In *2013 IEEE Aerospace Conference*, pages 1–12. IEEE, 2013.

[13] Robert P Mueller, Jonathan D Smith, Jason M Schuler, Andrew J Nick, Nathan J Gelino, Kurt W Leucht, Ivan I Townsend, and Adam G Dokos. Design of an excavation robot: regolith advanced surface systems operations robot (rassor) 2.0. In *ASCE Earth & Space Conference*, number STI NO. 25616, 2016.

[14] Hans Rickman. Composition and physical properties of comets. In *Solar System Ices: Based on Reviews Presented at the International Symposium "Solar System Ices" held in Toulouse, France, on March 27–30, 1995*, pages 395–417. Springer, 1998.

[15] Martin Rubin, Cécile Engrand, Colin Snodgrass, Paul Weissman, Kathrin Altwegg, Henner Busemann, Alessandro Morbidelli, and Michael Mumma. On the origin and evolution of the material in 67p/churyumov-gerasimenko. *Space science reviews*, 216(5):102, 2020.

[16] satsearch. A-str and aa-str. Accessed: February 14, 2024.

[17] satsearch. Cmg 40-60 s. Accessed: February 14, 2024.

[18] satsearch. Ibeos b28-1100 satellite battery. Accessed: February 14, 2024.

[19] satsearch. Smart sun sensor. Accessed: February 14, 2024.

[20] satsearch. Starlight 1000 iru. Accessed: February 14, 2024.

[21] Dong K. Shin and California Institute of Technology. Frequency and channel assignments. *DSN*, 201(810–005), Sep 2020.

[22] Fabio Caramelli Vittorio Bombelli, Ton Marée. Non-toxic liquid propellant selection method – a requirement-oriented approach. *41st AIAA/ASME/SAE/ASEE Joint Propulsion Conference & Exhibit*, 2005.

[23] Mike Wall. Spacex's starship: First crewed moon landing targeted for late 2025 or 2026, Year of publication (if available). Accessed: February 29, 2024.

[24] Wikipedia contributors. International space station, Year. Accessed: Date.